

Locality-Promoting Representation Learning

Johannes Schneider*
Institute of Information Systems
Vaduz, University of Liechtenstein
johannes.schneider@uni.li

June 7, 2022

Abstract

This work investigates fundamental questions related to locating and defining features in convolutional neural networks (CNN). The theoretical investigations guided by the locality principle show that the relevance of locations within a representation decreases with distance from the center. This is aligned with empirical findings across multiple architectures such as VGG, ResNet, Inception, DenseNet and MobileNet. To leverage our insights, we introduce Locality-promoting Regularization (LOCO-REG). It yields accuracy gains across multiple architectures and datasets.

1 Introduction

Feature engineering seems to be passé thanks to deep learning and its capability for end-to-end learning. Feature hierarchies are learnt automatically during the optimization of the loss function. That is, the following questions are answered without human intervention:

- Feature location estimate: “Which areas in an object constitute a feature?” (Q1)
- Feature strength estimate: “Given the location of a feature, how strongly is it present?” (Q2)

The two questions are intertwined, since a representation of a feature helps in answering both of them. The first question (Q1) is commonly discussed on a larger scale in a supervised manner, ie. object detection in images [19], where often a bounding box is extracted specifying the location of the object of interest. In convolutional neural networks, objects (or features) are not known a priori. The answer is also less explicit, since feature locations are not stated directly, but rather a feature map is computed. For each location the map contains a value stating the possibility or strength of a feature. Furthermore, a feature representation is spatially constrained to fixed dimensions, eg. width and height of 3×3 . The second question (Q2) assumes that the location of a feature is known and the goal is to assess feature strength, ie. whether the feature is present more or less prominently. The problem of feature strength estimation might be put as determining how much sub-features at different locations matter. For example, given a partially disassembled car after an accident the question becomes: How much of a car is this (still) if some parts are missing or deformed?

In our work, we address questions (Q1) and (Q2) by leveraging the Principle of Locality. Locality is a known theme in physics and in computer science, eg. [1]. In machine learning, CNNs or other fundamental primitives such as word-vectors [20] use some form of “locality”, ie. the idea that interaction strength decreases with distance. It justifies ignoring dependencies among data items, if their distances are above a threshold. Thus, “windows” or “patches” of inputs can be used as done for text in the context of deep learning [20] or images by CNNs. Prior work has motivated some ideas for representation learning based on principles from physics [2], but not using the Locality Principle.

This paper contributes by providing theoretical models inspired from physics for assessing the implications of locality on representation learning. Thereby, we address a call by Lake et al. [18] for grounding learning in physics. We find that under the assumption of locality and the demand for cohesive features, elements of a

*Work conducted during extra hours

feature representation that are close to its center are more relevant. The theoretical finding is supported by empirical evidence through investigating learnt features of multiple architectures. Our locality promoting L2-regularization scheme (“LOCO-REG”) for exploiting locality results in improvements across multiple architectures such as ResNet, VGG and MobileNet. Furthermore, as a by-product, LOCO-REG provides a new type of architectural element being a compromise between (spatial) $k \times k$ convolutions and $j \times j$ convolutions with $j \neq k$. For example, dependent on the regularization parameters, a 3×3 convolution using LOCO-REG might resemble more of a 1×1 convolution or be closer to a 3×3 convolution with ordinary L2-regularization. Our perspective based on the Locality Principle also provides novel insights and ways of interpretation for deep learning. For example, it allows to interpret shortcuts as popularized in ResNet-style networks [13] as locality promoting.

2 Related Work

Some priors for “what makes a good representation” have been briefly motivated by physics [2]. Locality or the idea of emphasizing the center of a representation has not been discussed. The closest weakly related idea is spatial coherence, which is said to imply slow changes of features across spatial dimensions. Locality implies that relevance of feature weights decrease with distance from the center. Disentangling of features is also an important aspect in representation learning. Works on feature disentanglement [27, 23] often constrain representations, eg. weight matrices might be enforced to be orthogonal [23]. These works aim at reducing the number of similar representations. Our approach does not directly constrain representations to be dissimilar, but it may encourage locating features (and inferring representations) at positions that are spatially separated - see Table 3. Since interactions decrease with distance, larger spatial separation might imply more differences in inputs. Thus, one might hope for obtaining more distinct feature representations compared to the ones that are learnt using patches of nearby or overlapping data.

Precise location of features has not been deemed essential in the early stages of deep learning. Early works [21] on image recognition as well as more recent architectures such as inception [26] or VGG [24] might use max-pooling that neglects spatial information by simply extracting the maximum out of a region without keeping any information on its position within the considered region. However, it has been recognized that operations such as convolutions [25] or fractional max-pooling [11] that allow to maintain spatial information more accurately are more suitable for down-sampling. Pooling has been seen as a mechanism to achieve (more) translation invariance. More elaborate approaches such as spatial transformer networks [16] allow to learn multiple transformations such as shear, translation and scaling. There is a significant body of work that discusses invariance, e.g. [8, 4]. [8] showed how to exploit groups of symmetries such as rotations and reflections. These works aim at replacing the learning of (many) transformable representations, by learning the transformation itself and (fewer) representations on which the transformation can be applied. In contrast, we are more concerned with defining individual representations well rather than reducing the number of representations.

Our work is also loosely related to aspects of the human visual system. Lateral inhibition is an effect, where neurons suppress their less-active neighbors [21, 22]. For instance, it plays a key role for Mach bands, where they increase the contrast between different tones of gray, ie. neurons perform high pass filtering. Our work is neither limited to high pass filtering nor do we strongly inhibit features. But for our implementation we also train features by slightly reducing the impact of outer parts of a feature, ie. the sub-features of which it is composed, to compensate for the promotion of the center.

There are many regularization schemes, such as L1- and L2-regularization, elastic nets [30] or versions of dropout such as dropconnect [28]. Other works have also used regularization as a means to achieve desired properties of feature representations, eg. regularization in [23] pushes pairs of kernels towards a small cosine metric, ie. towards being orthogonal. In contrast, we focus on regularization of elements of a representation rather than pairs of complete representations.

3 Locality Principle

A hierarchy of features is an intuitive concept, since any physical object can be decomposed into smaller parts. Each part might be an object itself. Physical objects often appear easy to localize due to well-recognizable

boundaries. Features are often harder to pinpoint. A feature map might be interpreted as a probability of a “feature” (or object) at a specific location or as the “strength” of a feature at that location. For example, in Figure 1 a white pixel could be said to indicate a probability of 1 that a feature is present and a black pixel could indicate a probability of zero. As can be seen, mostly transitions between high and low probabilities are smooth – in particular for layers closer to the input. Therefore, to answer Question (Q1), ie. estimating the exact location from the feature map giving probabilities, it seems reasonable to take these insights into account by proclaiming that a feature should be located in areas with overall high probability and, therein, possibly centered at peaks, ie. local maxima. As we shall see, locality fosters locating features at such locations. The

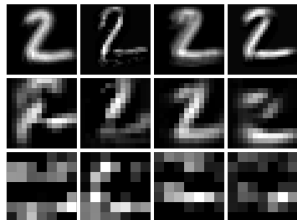


Figure 1: Four feature maps for each of the three layers of a simple CNN. It indicates that features often appear and disappear gradually. More so in lower layers.

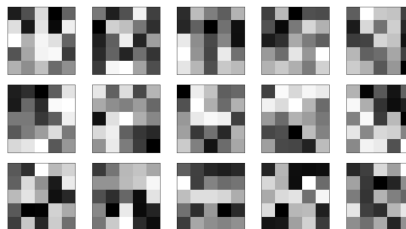


Figure 2: Randomly chosen filters of the CNN used for Figure 1. While barely visible at best, locations closer to the center have larger weights, ie. are brighter, on average.

second question (Q2) is concerned with the problem of defining a feature in terms of sub-features. Given a location of the feature and feature maps describing the degree of presence of the lower-level features, an answer to the second question demands computing how strongly the feature “exists”. Under the assumption of locality, interactions of nearby parts of a feature matter more than between distant ones. For example, in an image nearby pixels bear more similarity than distant pixels. For feature strength estimation, locality combined with cohesion requirements of features, leads to the statement that locations of a feature near its center matter more than those near its boundary. Figure 2 highlights the weights of a few filters, ie. features. The locality principle implies that locations closer to the center should be brighter. While this is poorly visible (if at all), we show empirically in Section 7.1 that there are significant differences.

4 Feature Localization

Feature localization aims at identifying the boundary of a feature, e.g. width and height of a bounding box and the position of the box that is supposed to contain a feature. CNNs have representations of fixed dimensions, ie. fixed width and height of filters. Thus, the problem becomes finding the position (of the center). Generic ideas, eg. found in [2], might be applied and extended to the problem of locating features within feature maps. That is, for position estimates of features should hold:

- Well-separated (Section 4.1): Feature maps representing feature locations should be non-uniform, having strict maximas at distant locations. This relates to cohesion of features.
- Robust to noise (Section 4.2): Random changes in inputs should not change feature locations

4.1 Feature Separation And Cohesion

We show that locality combined with the objective of obtaining cohesive features implies that the more central a location of a feature is, the more relevant it is. Though each part interacts with every other part, the center has more short-range interactions. Since they are stronger, the center is more important to obtain a cohesive unit (see right part of Figure 4). Thus, it is preferable to locate a feature at positions in the feature map where the value (or strength) of the center is big, though all parts of a feature matter. For illustration, consider the task of locating two 3×3 features given just a single data sample shown in Figure 3. Since most values are small, ie. 0 or 1, and potentially superimposed by noise, features seem to be present where the values of the feature maps are large. Figure 3 shows the outcomes of two strategies. The strategy that

0	0	0	0	0	1	1	0	0	1	1	0	0	0	0	
0	0	1	0	0	1	2	2	1	0	2	3	1	1	1	0
1	0	0	0	1	2	6	3	1	1	2	5	1	2	1	0
0	0	0	0	1	1	3	2	2	3	2	3	2	0	0	0
0	1	0	0	0	1	2	2	2	2	3	2	2	1	0	0
0	0	0	1	0	1	1	1	2	3	3	2	1	1	0	0

Figure 3: Input and localized 3×3 features. The two red features are defined using the locality principle and the blue ones by maximizing the sum of inputs.

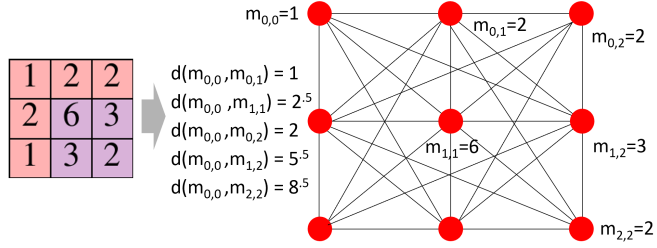


Figure 4: Interpretation of parts of a feature map as interacting particles. Particles are red points with exemplary masses according to the left part of the figure (extracted from Figure 3). Lines indicate interactions.

treats all parts of a proposed feature uniformly places features so that the aggregated sum of inputs covered by the feature is maximal (blue features). The other strategy adhering to locality places more importance on the center, ie. the center should be large (red features). Feature positions determined using the locality adhering principle seem to be more robust to certain forms of changes of the input. To make our point more credible, we provide models derived from physics yielding a more concise and deeper understanding under the assumption of locality and the objective of cohesive features.

As in clustering, ideally features are dense, ie. positioned at areas with high density, and well-separated as captured by cluster assessment metrics like the Davies-Bouldin Index that computes the deviation of the center of a cluster to its members and distances between clusters. Cohesion relates naturally to density and it implies that a feature is stable. We seek to locate a feature of fixed dimension, ie. 3×3 , so that cohesion is maximal. Our cohesion metric relies on a form of attraction analogous to “gravity” that has also been used in the context of clustering [12, 5]. We formulate the objective of obtaining highly cohesive features by demanding that feature parts should maximize their attraction. We use the common idealization of point masses, meaning that we neglect the spatial extension of parts of a feature and subsume their strength at a single point (Figure 4). Attraction or force between masses at locations (i, j) and (k, l) might be measured analogous to gravity $F(m_{i,j}, m_{k,l}) := c_0 \frac{m_{i,j} \cdot m_{k,l}}{d(m_{i,j}, m_{k,l})^q}$, where c_0 is a constant (as for gravity), $m_{i,j}$ can be seen as the mass or absolute strength of a feature at a location, d is the Euclidean distance and $q > 0$ a parameter, eg. we shall use $q = 2$ as for gravity. This scenario is illustrated in Figure 4. The goal is to identify features at locations in the feature map that are strongly cohesive.¹

Cohesion might be measured using the sum of all interactions, i.e. the sum of forces among each pair of parts, ie. $F_{tot} := \sum_{i,j,k,l} F(m_{i,j}, m_{k,l})$ with the force on parts themselves being defined as 0, ie. $F(m_{i,j}, m_{i,j}) := 0$. We compute distances by taking the differences between indexes, $d(m_{i,j}, m_{k,l}) := \sqrt{(i-k)^2 + (j-l)^2}$. Any distance is only proportional to the actual (physical) distance with some proportionality constant c_1 , which can be subsumed in the constant c_0 in the force $F(m_{i,j}, m_{k,l})$.

Theorem 1. *For any feature strength distribution $m' \leq m_c, m_{co}, m_n < (1 + \epsilon)m'$ with $\epsilon \in [0, 0.675]$, the cohesion F_{tot} of the feature is increased most by increasing m_c , and more by increasing any $m_n \in M_n$ than any $m_{co} \in M_{co}$ for arbitrary m' , center $m_c = m_{1,1}$, direct neighbors $M_n := \{m_{1,0}, m_{0,1}, m_{2,1}, m_{1,2}\}$ and corners $M_{co} := \{m_{0,0}, m_{2,0}, m_{2,2}, m_{0,2}\}$ (Figure 4).*

The theorem follows essentially from the fact that the center has (on average) smaller distances to other masses making its contribution to overall cohesion the largest. Analogously, any direct neighbor of the center has (on average) smaller distances to other masses than any corner.

Proof. We consider the dependency of the total force F_{tot} on the center m_c , a corner mass m_{co} and a direct neighbor mass m_n using case enumerations. That is, we investigate the impact on the total force if one of them is changed. Any interaction not involving any of the masses m_c, m_n or m_{co} can be neglected, since

¹In feature maps values can be negative, whereas the existence of negative masses are unclear. Thus, the analogy to physical masses needs clarification. Many activation functions limit negative feature strength, eg. ReLu enforces a lower bound of zero. Standardization (BatchNorm) after ReLu may cause negative values, but it can also be done before ReLu with limited impact. More importantly, BatchNorm is optional. As such, one may assume non-negative feature maps.

it is not impacted by altering the three masses. Furthermore, due to symmetry only few cases need to be considered.

First, we prove that increasing the center $m_{1,1}$ yields larger change than changing a corner $m_{0,0}$ or direct neighbor $m_{0,1}$. We consider the contribution F_c of the center mass $m_{1,1}$ to F_{tot} , ie. all interactions that involve $m_{1,1}$ (see Equations 4.1), as well as the contribution F_{co} of the corner mass $m_{0,0}$ and the contribution F_n of the direct neighbor mass $m_{0,1}$. The cases for changing any other mass $m_{i,j}$ are symmetric. The forces can be computed by using the distances shown in Figure 4. As shown, due to symmetry there are only 4 different distances $1, \sqrt{2}, 2, \sqrt{5}, \sqrt{8}$.

$$\begin{aligned}
F_c &:= \sum_{k,l} F(m_{1,1}, m_{k,l}) = c_0 \cdot m_{1,1} \cdot \left(\sum_{m \in M_n} m + \frac{\sum_{m \in M_{co}} m}{\sqrt{2}^q} \right) \\
F_n &:= \sum_{k,l} F(m_{0,1}, m_{k,l}) = c_0 \cdot m_{0,1} \cdot \left(m_{1,1} + \left(\frac{m_{1,0} + m_{1,2}}{\sqrt{2}^q} + \frac{m_{2,1}}{2^q} \right) + \left(m_{0,0} + m_{0,2} + \frac{m_{2,0} + m_{2,2}}{\sqrt{5}^q} \right) \right) \\
F_{co} &:= \sum_{k,l} F(m_{0,0}, m_{k,l}) = c_0 \cdot m_{0,0} \cdot \left(\frac{m_{1,1}}{\sqrt{2}^q} + \left(m_{0,1} + m_{1,0} + \frac{m_{2,1} + m_{1,2}}{\sqrt{5}^q} \right) + \left(\frac{m_{2,0} + m_{0,2}}{2^q} + \frac{m_{2,2}}{\sqrt{8}^q} \right) \right)
\end{aligned} \tag{4.1}$$

Next, we substitute $q = 2$ and we compute the impact on the total force when changing one of the three chosen masses, ie. $m_{1,1}$, $m_{0,1}$ and $m_{0,0}$.

$$\begin{aligned}
\frac{dF_c}{dm_{1,1}} &= c_0 \cdot \left(\sum_{m \in M_n} m + \frac{\sum_{m \in M_{co}} m}{2} \right) \\
\frac{dF_n}{dm_{0,1}} &= c_0 \cdot \left(m_{1,1} + \left(\frac{m_{1,0} + m_{1,2}}{2} + \frac{m_{2,1}}{4} \right) + \left(m_{0,0} + m_{0,2} + \frac{m_{2,0} + m_{2,2}}{5} \right) \right) \\
\frac{dF_{co}}{dm_{0,0}} &= c_0 \cdot \left(\frac{m_{1,1}}{2} + \left(m_{0,1} + m_{1,0} + \frac{m_{2,1} + m_{1,2}}{5} \right) + \left(\frac{m_{2,0} + m_{0,2}}{4} + \frac{m_{2,2}}{8} \right) \right)
\end{aligned} \tag{4.2}$$

We begin with comparing the change of the center to that of the direct neighbor $m_{0,1}$, ie. we start by showing that

$$\frac{dF_c}{dm_{1,1}} > \frac{dF_n}{dm_{0,1}} \tag{4.3}$$

We prove inequality (4.3) by showing that even under a ‘‘worst-case’’ distribution of masses the inequality holds. By assumption for any mass $m_{i,j}$ holds $m_{i,j} \in [m', (1+\epsilon)m']$. Let us minimize the left hand side ($\frac{dF_c}{dm_{1,1}}$) and maximize the right hand side ($\frac{dF_n}{dm_{0,1}}$). Formally, we can consider coefficients for masses in Equations 4.2. If a coefficient for a mass in $\frac{dF_n}{dm_{0,1}}$ is larger than in $\frac{dF_c}{dm_{1,1}}$ then the corresponding mass should be maximized, otherwise minimized. More intuitively, enlarging the mass at location i, j increases F_n more than F_c if one of the two conditions holds: (i) if location i, j is closer to the neighbor $(0, 1)$ than to the center and (ii) if $\frac{dF_n}{dm_{0,1}}$ depends on location i, j but $\frac{dF_c}{dm_{1,1}}$ does not. Condition (i) only applies to the two corners $(0, 0)$ and $(0, 2)$ that are nearest to $m_{0,1}$. That is, these two corners should have maximal masses $(1+\epsilon)m'$. For condition (ii) note that the increase of F_n depends on the center $m_{1,1}$ (but not on $m_{0,1}$), whereas the change of F_c does not depend on $m_{1,1}$ but on $m_{0,1}$. Thus, the center mass should be maximal, ie. $m_{1,1} = (1+\epsilon)m'$, and all others, including $m_{0,1}$, are minimized, ie. set to m' . Substituting the suggested masses into Equations 4.2 gives:

$$\begin{aligned}
\frac{dF_c}{dm_{1,1}} &= c_0 \cdot \left(4m' + \frac{2m' + 2(1+\epsilon)m'}{2} \right) = c_0 m' (6 + \epsilon) \\
\frac{dF_n}{dm_{0,1}} &= c_0 \cdot \left((1+\epsilon)m' + 1.25m' + ((2+\epsilon)m' + 0.4m') \right) = c_0 m' (4.65 + 3\epsilon)
\end{aligned}$$

Setting the two terms, ie. $\frac{dF_c}{dm_{1,1}}$ and $\frac{dF_n}{dm_{0,1}}$, equal gives $\epsilon = 0.675$, ie. the bound is $\epsilon < 0.675$.

An analogous consideration for the corner mass $m_{0,0}$, ie. investigating if $\frac{dF_c}{dm_{1,1}} > \frac{dF_{co}}{dm_{0,0}}$, yields that in contrast to the direct neighbor $m_{0,1}$, for the corner $m_{0,0}$ there are no masses closer to the corner. Thus, this case is subsumed by the prior case for $m_{0,1}$ stated in Inequality 4.3, ie. the prior bound $\epsilon < 0.675$ also applies.

Next, we show that changing any of the direct neighbors M_n has greater impact on cohesion, ie. F_{tot} , than changing any of the corners M_{co} . Due to symmetry it suffices to consider only one mass in M_n , ie. we chose $m_{0,1}$, and two corners, ie. we use $(0, 0)$ and $(2, 0)$. We begin by showing that increasing the mass of neighbor $(0, 1)$ has more impact than changing the corner $m_{0,0}$. That is, we show $\frac{dF_n}{dm_{0,1}} > \frac{dF_{co}}{dm_{0,0}}$. The derivatives are given in Equations 4.2.

Let us minimize the left hand side ($\frac{dF_n}{dm_{0,1}}$) and maximize the right hand side ($\frac{dF_{co}}{dm_{0,0}}$). $\frac{dF_n}{dm_{0,1}}$ is minimized and $\frac{dF_{co}}{dm_{0,0}}$ maximized if masses closer to $m_{0,0}$ are maximized or those which only occur with positive coefficient in $\frac{dF_{co}}{dm_{0,0}}$. This means $m_{0,1}$, $m_{1,0}$ and $m_{2,0}$ are chosen to be maximal, ie. they are set to $(1 + \epsilon)m'$ and other masses are minimized, ie. set to m' .

$$\begin{aligned}\frac{dF_n}{dm_{0,1}} &= c_0(m' + 0.5m' + 0.5(1 + \epsilon)m' + 0.25m') + 2m' + 0.2(1 + \epsilon)m' + 0.2m' = c_0m'(4.65 + 0.7\epsilon) \\ \frac{dF_{co}}{dm_{0,0}} &= c_0(0.5m' + 2(1 + \epsilon)m' + 0.4m' + 0.25(1 + \epsilon)m' + 0.25m' + 0.125m') = c_0m'(3.525 + 2.25\epsilon)\end{aligned}$$

Setting the two terms, ie. $\frac{dF_n}{dm_{0,1}}$ and $\frac{dF_{co}}{dm_{0,0}}$, equal gives: $1.125 = 1.55\epsilon$, ie. $\epsilon = 0.725\dots$

Finally, we consider the more distant corner $m_{2,0}$. We show $\frac{dF_n}{dm_{0,1}} > \frac{dF_{co}}{dm_{2,0}}$. The derivative $\frac{dF_n}{dm_{0,1}}$ is given in Equations 4.2. For $\frac{dF_{co}}{dm_{2,0}}$ we have

$$\frac{dF_{co}}{dm_{2,0}} = c_0\left(\frac{m_{1,1}}{2} + (m_{2,1} + m_{1,0} + \frac{m_{0,1} + m_{1,2}}{5}) + (\frac{m_{2,2} + m_{0,0}}{4} + \frac{m_{0,2}}{8})\right)$$

Let us minimize the left hand side ($\frac{dF_n}{dm_{0,1}}$) and maximize the right hand side ($\frac{dF_{co}}{dm_{2,0}}$). As before, $\frac{dF_n}{dm_{0,1}}$ is minimized and $\frac{dF_{co}}{dm_{2,0}}$ maximized if masses closer to $m_{0,0}$ are maximized or those which only occur with positive coefficient in $\frac{dF_{co}}{dm_{2,0}}$, ie. $m_{0,1}$, $m_{1,0}$, $m_{2,1}$ and $m_{2,2}$ are maximal, ie. they are set to $(1 + \epsilon)m'$ and other masses are minimized, ie. set to m' . This gives:

$$\begin{aligned}\frac{dF_n}{dm_{0,1}} &= c_0(m' + (0.5m' + 0.75(1 + \epsilon)m') + 2m' + 0.2(1 + \epsilon)m' + 0.2 = c_0m'(4.65 + 0.95\epsilon) \\ \frac{dF_{co}}{dm_{2,0}} &= c_0(0.5m' + 2(1 + \epsilon)m' + 0.2(1 + \epsilon)m' + 0.2m' + 0.25(1 + \epsilon)m' + 0.25m' + 0.125m') \\ &= c_0m'(3.525 + 2.45\epsilon)\end{aligned}$$

Setting the two terms equal gives $\epsilon = 1.125/1.5 = 0.75$. Thus, the bound that is valid for all cases is given by $\epsilon < 0.675$. □

The theorem shows that for many distributions of masses cohesion depends more on masses near the center, ie. increasing any of them yields larger gains in cohesion than masses far away from the center. Thus, features should be centered, where the feature map exhibits larger values. Locality is incorporated in the definition F_{tot} stating a decrease of interactions with distance. The provided bounds in the theorem might not be tight, but irrespective of this, there are (pathological) cases of feature strength distributions so that enlarging the center might not increase cohesion more than enlarging other parts. For example, assume a corner mass, eg. $m_{0,0}$, is much bigger than any other mass. Then, growing the mass of one of its direct neighbors, eg. $m_{0,1}$, can lead to a more cohesive solution than growing the center $m_{1,1}$. This follows since the center has larger distance to the corner.

4.2 Noise And Sharpening

Assume that inputs to a layer are noisy and our goal is to locate a feature on a feature map, ie. infer the position given that the feature map is influenced by noise. There are numerous types of noise, particularly well known in images are, for example, salt and pepper, one-shot, quantization and Gaussian noise [3]. Sources of noise might be the data as well as the estimation process. Our focus is not primarily on removal of noise in the data fed into the network, ie. into the first layer, but rather in noise in the input of any layer. Noise might be present in a smooth manner as defining the uncertainty of the area, where a feature is located. We might say that a feature is almost certainly within a coherent area, but it is hard to localize exactly therein. Noise might also be strongly varying across locations such as Gaussian noise, ie. uncorrelated noise being identically independently distributed. In our model we use Gaussian noise, since it is common and we deem some kinds of noise as fairly unlikely or irrelevant. Quantization noise, for example, might have little impact in deep learning since lower quantization of weights can yield very good results, eg. [9]. Gaussian noise can be removed using Gaussian Filters [10]. It is plausible to use filters for denoising and sharpening as a ‘‘preprocessing’’ step. Such filters have larger weights in the center (see Table 1). Furthermore, it is also known that first layer filters in

neural networks resemble common filters such as edge detectors or Gabor Filters [7]. However, our objective is not the removal of noise, but rather finding robust feature locations given noise. To get a conceptual

Table 1: Filters for Denoising and Sharpening

Gaussian	<table style="border-collapse: collapse; margin: auto;"> <tr><td style="padding: 2px 5px;">.06</td><td style="padding: 2px 5px;">.12</td><td style="padding: 2px 5px;">.06</td></tr> <tr><td style="padding: 2px 5px;">.12</td><td style="padding: 2px 5px;">.25</td><td style="padding: 2px 5px;">.12</td></tr> <tr><td style="padding: 2px 5px;">.06</td><td style="padding: 2px 5px;">.12</td><td style="padding: 2px 5px;">.06</td></tr> </table>	.06	.12	.06	.12	.25	.12	.06	.12	.06	Laplacian	<table style="border-collapse: collapse; margin: auto;"> <tr><td style="padding: 2px 5px;">-1</td><td style="padding: 2px 5px;">-1</td><td style="padding: 2px 5px;">-1</td></tr> <tr><td style="padding: 2px 5px;">-1</td><td style="padding: 2px 5px;">8</td><td style="padding: 2px 5px;">-1</td></tr> <tr><td style="padding: 2px 5px;">-1</td><td style="padding: 2px 5px;">-1</td><td style="padding: 2px 5px;">-1</td></tr> </table>	-1	-1	-1	-1	8	-1	-1	-1	-1
.06	.12	.06																			
.12	.25	.12																			
.06	.12	.06																			
-1	-1	-1																			
-1	8	-1																			
-1	-1	-1																			

understanding, we derive a solution for weights for an one dimensional feature map with the goal of locating a single feature. The feature map is defined as $m(x) := g(x) + \epsilon_x$ for integer x . It is the superposition of the true undistorted feature strength distribution g and a random variable ϵ_x , so that all ϵ_j are independently identically distributed with mean 0, ie. $E[\epsilon_j] := 0$ and variance $\text{Var}(\epsilon_j) := s^2$. We seek to find the location x^* with the strongest indication of a feature according to the feature map g . Suppose w.l.o.g. that the feature to be found is located at $x^* = 0$. We assume that the feature strength follows locality. That is, feature strength is maximal at 0 and it decreases with distance from 0. Formally, let g be symmetric, ie. $g(x) = g(-x)$ and assume that $g(x) > g(x + 1)$ for $x \geq 0$ and $g(x) > g(x - 1)$ for $x \leq 0$. We also assume that the decrease is strongest close to the maximum, ie. $g(x) - g(x + 1) > g(x + 1) - g(x + 2)$ for $x \geq 0$ and analogously for $x \leq 0$, $g(x) - g(x - 1) > g(x - 1) - g(x - 2)$. We consider a 1d convolution $f(x, w) := \sum_{j=-k}^k w_j \cdot m(x + j)$. Thus, convolutions are of odd length, ie. $2k + 1$ and centered at zero. Given w the estimated location x' is at the maximum of the convoluted feature map, ie. $x' := \arg \max_x f(x, w)$. Desirable properties of f include that $f(x, w)$ is maximal at the true feature location x^* and smaller at other locations. In fact, we might demand that there is a clear gap between the estimate at the maximum x^* and other locations. That is, like in game theory we conduct a “minimax” optimization $\min_{x \neq x^*} \max_w E[f(x^*, w) - f(x, w)]$. This worst-case optimization means that weights w are chosen first so that a subsequent minimization by selecting x yields maximum value. The estimator should also have small variance $\text{Var}(f(x, w) - f(x^*, w))$.

Theorem 2. *The objective $\min_{x \neq x^*} \max_w E[f(x^*, w) - f(x, w)]$ is maximized for $w_0 > 0$ and $w_{-1} = w_1 = 0$. The variance is $\text{Var}(f(x, w) - f(x^*, w)) = s^2 \sum_{j=-k}^k w_j^2$. If weights are constraint, ie. $\sqrt{\sum_j w_j^2} = 1$, it is minimized for uniform weights $w_j = 1/\sqrt{2k + 1}$ for all j .*

The theorem highlights the trade-off between variance and expectation, ie. the best solution for variance is non-optimal for expectation and the other way around. Qualitatively, increasing noise, ie. $\text{Var}(\epsilon_x) = s^2$, fosters more uniform weights. Stronger concentration of the maximum, ie. having faster decrease of g with distance, fosters a larger center weight. We conclude that up to a certain noise level, the center weight w_0 should be larger than the surrounding weights w_j for $j \neq 0$.

Proof. For the variance holds:

$$\begin{aligned}
 \text{Var}(f(x, w) - f(x^*, w)) &= \text{Var}\left(\sum_{j=-k}^k w_j \cdot g(x + j) - \sum_{j=-k}^k w_j \cdot g(j)\right) \\
 &= \text{Var}\left(\sum_{j=-k}^k w_j \cdot g(x + j) + \sum_{j=-k}^k w_j \epsilon_{x+j} - \sum_{j=-k}^k w_j \cdot g(j)\right) \\
 &= \text{Var}\left(\sum_{j=-k}^k w_j \epsilon_{x+j}\right) = \sum_{j=-k}^k w_j^2 \text{Var}(\epsilon_{x+j}) = s^2 \sum_{j=-k}^k w_j^2
 \end{aligned}$$

The solution minimizing the variance with weights of fixed norm, ie. 1, is obtained for uniform weights, e.g. $w_j = 1/\sqrt{2k + 1}$.

For the expectation holds:

$$\begin{aligned}
\mathbb{E}[f(x^*, w) - f(x, w)] &= \mathbb{E}[f(0, w) - f(x, w)] = \mathbb{E}\left[\sum_{j=-k}^k w_j \cdot (g(j) - g(x+j) + \epsilon_j - \epsilon_{x+j})\right] \\
&= \sum_{j=-k}^k w_j \cdot (\mathbb{E}[g(j) - g(x+j)] + E[\epsilon_j - \epsilon_{x+j}]) \quad \text{using linearity of expectation} \\
&= \sum_{j=-k}^k w_j \cdot (g(j) - g(x+j) + E[\epsilon_j] - E[\epsilon_{x+j}]) \\
&= \sum_{j=-k}^k w_j \cdot (g(j) - g(x+j)) \quad \text{since } \mathbb{E}[\epsilon_i] := 0
\end{aligned}$$

Thus, we get:

$$\begin{aligned}
\min_{x \neq x^*} \max_w \mathbb{E}[f(x^*, w) - f(x, w)] &= \min_{x \neq x^*} \max_w \sum_{j=-k}^k (g(j) - g(x+j)) \cdot w_j \\
&= \min_{x \neq x^*} \max_w (g(-1) - g(x-1)) \cdot w_{-1} + (g(0) - g(x)) \cdot w_0 + (g(1) - g(x+1)) \cdot w_1
\end{aligned} \tag{4.4}$$

From $g(x) - g(x+1) > g(x+1) - g(x+2)$ and $g(x) > g(x+1)$ for $x \geq 0$ follows

$$g(a) - g(a+c) > g(b) - g(b+d) \text{ for } b > a \geq 0 \text{ with } c \geq d > 0 \tag{4.5}$$

Analogously, from $g(x) - g(x-1) > g(x-1) - g(x-2)$ and $g(x) > g(x-1)$ for $x \leq 0$ follows

$$g(a) - g(a-c) > g(b) - g(b-d) \text{ for } 0 \geq a > b \text{ with } c \geq d > 0 \tag{4.6}$$

Equations 4.5, 4.4 and symmetry of g , ie. $g(x) = g(-x)$, are used to derive Table 2.

Table 2: Coefficients in Equation 4.4 for different x

	Coefficients for		
	w_{-1}	w_0	w_1
x	$g(-1) - g(x-1)$	$g(0) - g(x)$	$g(1) - g(x+1)$
-3	$g(1) - g(4) > 0$	$g(0) - g(3) > 0$	$g(1) - g(2) > 0$
-2	$g(1) - g(3) > 0$	$g(0) - g(2) > 0$	$g(1) - g(1) = 0$
-1	$g(1) - g(2) > 0$	$g(0) - g(1) > 0$	$g(1) - g(0) < 0$
1	$g(1) - g(0) < 0$	$g(0) - g(1) > 0$	$g(1) - g(2) > 0$
2	$g(1) - g(1) = 0$	$g(0) - g(2) > 0$	$g(1) - g(3) > 0$
3	$g(1) - g(2) > 0$	$g(0) - g(3) > 0$	$g(1) - g(4) > 0$

We investigate properties of solutions w that maximizes the objective (4.4) using Table 2 for all x . Let's consider solutions for $|x| \geq 2$. The coefficient for w_0 is always positive and largest (in magnitude) for all listed x in Table 2 using Equation 4.5 with $a = 0$, $b = 1$. This also holds for $|x| \geq 4$ by doing an inductive step from x to $x+1$ for $x > 3$ and x to $x-1$ for $x < -3$. That is, for $x > 3$ we have $g(0) - g(x) > g(1) - g(1+x) > g(1) - g(x-1)$ using Equation 4.5. Analogously for $x < -3$ and for x to $x-1$ holds $g(0) - g(x) > g(-1) - g(x-1) > g(-1) - g(x-1)$ using Equation 4.6. Thus, it is best to maximize w_0 and set w_{-1} and w_1 to 0.

Assume that $|x| = 1$. Consider any solution for w that is optimal for $x = -1$. If $w_1 > 0$ the solution would not be optimal since the coefficient $g(1) - g(0)$ is negative. Thus, assume $w_1 \leq 0$. Furthermore, assume that $w_{-1} \geq 0$ (otherwise the solution would also not be optimal for $x = -1$). In the same manner as for $x = -1$, for $x = 1$ follows $w_1 \geq 0$ and $w_{-1} \leq 0$. Thus, the only situation where a solution is neither improvable for $x = -1$ nor $x = 1$, ie. optimal for both, is if $w_1 = w_{-1} = 0$. In any other case, the solution could be improved by shifting w_1 and/or w_{-1} closer to 0.

□

5 Feature Strength and Locality

Feature strength is determined by computing a value indicating the feature’s presence based on the occurrence of sub-features in a feature hierarchy. We assume that a location specifying the center of the feature is known and that the feature is of fixed, known dimensions. Locality implies that interactions decrease with distance. Thus, sub-features further from the center should matter less in defining the feature. To make this more graspable, suppose a picture of a flower, constituting a feature to be learnt, is given. Locality might imply that to define the feature strength one should look carefully at the center of the flower and less at the outer parts of it, eg. its leaves. (This is in contrast to considering all parts of the entire flower equally.). Note, that we do not claim (or show) that this is valid for all features. Here, we only ascertain the implications of locality. More formally, we assume that we aim to maximize the alignment of a pattern represented by w and the actual feature as present in the feature map m . We want to find weights that optimize $\min_w \sum_{j=-k}^k \|m(j) \cdot l(j) - w_j\|_p$ for some L_p norm with the function l quantifying the degree to which features near the center matter more, ie. we have $l(x) > l(x+1)$ for $x \geq 0$ and $l(x) > l(x-1)$ for $x \leq 0$. It is easy to see that the optimal solution is $w_j = m(j)l(j)$. This solution implies that given all sub-features are equally strongly present, ie. $m(j) = m(i)$, weights near the center should be larger.

6 Locality-Promoting Regularization (LOCO-REG)

Assuming locality, the learning process should encourage feature representations that reflect locality and foster cohesive features. This means weights near the center should be larger. One mechanism to guide the learning process in this direction is to use regularization. Weights are regularized depending on their distance to the center. Regularization also allows for features, where the largest weight is not in the center, which is commonly observed. The conventional overall regularization parameter λ is adjusted by a factor $g(i, j)$ depending on location i, j . It is convenient to constrain $g(i, j)$, so that $\sum_{i,j} g(i, j) = 1$. This implies that the effect of the non-uniform spatial regularization due to $g(i, j)$ only impacts the distribution of the regularization strength for different weights but not the total amount of regularization given by λ . Thus, the parameter λ provides the overall magnitude of regularization. For a $k \times k$ matrix $w_{i,j}$ of a filter being convoluted with some feature map, the term added to the loss function becomes $\lambda(\sum_{i,j} g(i, j) \|w_{i,j}\|_p)$, where $p = 1$ implies L1-regularization and $p = 2$ corresponds to L2-regularization. For brevity in notation, we focus on the 3×3 case for L2-regularization. We use a symmetric function g , ie. all corners are regularized identically based on a parameter η , the center is regularized with a parameter γ and all direct neighbors of the center are regularized with the same constant. More precisely, whereas uniform L2-regularization adds $\lambda \|w_{i,j}\|_2^2 = \lambda w_{i,j}^2$ to the loss function, the suggested LOCO-REG (LOcality-prOmoting REGularization) loss for each spatial filter $w_{i,j}$ with normalization constant Z , corner indexes I_{co} and nearest neighbors I_n is:

$$\begin{aligned} \text{LOCO-REG Loss} &:= L_2^{\text{Reg.Loss}}(w_{i,j}) = \frac{\lambda}{Z} (\gamma w_{1,1}^2 + \sum_{(i,j) \in I_n} w_{i,j}^2 + \sum_{(i,j) \in I_{co}} \eta w_{i,j}^2) \\ Z &:= \frac{\gamma + 4(1 + \eta)}{9} \quad I_n := \{(0, 1), (1, 0), (1, 2), (2, 1)\} \quad I_{co} := \{(0, 0), (2, 0), (0, 2), (2, 2)\} \end{aligned} \tag{6.1}$$

7 Experiments

We provide empirical support for locality and highlight the performance of LOCO-REG. We assess three networks: VGG and MobileNet variants (Table 3) as well as ResNet-18 [13]. They cover different design ideas, such as stacking many convolutional layers (VGG), using shortcuts (ResNet) and separating spatial and depth-wise convolutions (MobileNet).

For all experiments we trained for 250 epochs decaying the initial learning rate of 0.1 by 0.316 after epochs 70, 140, 190, 230, 245. We used SGD with momentum 0.9 and batchsize 128. For each dataset, ie. CIFAR-10, CIFAR-100 [17] and FASHION-MNIST [29] (scaled to (32,32)), 10000 samples were used for testing and the rest for training. Data augmentation consisted of horizontal flipping and random 8×8 image cropping. For (overall) L2-regularization we used $\lambda = 0.0005$. We used TensorFlow, training on multiple servers using NVidia’s 1080 and 2080 GPUs. We conducted 20 runs for each dataset and architecture for LOCO-REG and uniform (standard) regularization, ie. $(\gamma, \eta) = (1, 1)$.

Table 3: Architectures, where ‘‘C’’ is a convolutional, ‘‘Soft’’ a Softmax and ‘‘MP’’ a MaxPool layer; a BatchNorm and a ReLu layer followed each ‘‘C’’ layer. The supplementary material contains TensorFlow models.

MobileNet Adaption [14]		VGG13 Adaption [24]		Continued...			
Type/Stride	Filter Shape	Type/Stride	Filter Shape	C/s1	1×1×256×256	C/s1	3×3×3×512
C/s1	3×3×3×64	C/s1	3×3×3×64	C dw/s2	3×3×256	MP/s2	Pool 2×2
C dw/s2	3×3×64	C/s1	3×3×3×64	C/s1	1×1×256×256	C/s1	3×3×3×512
C/s1	1×1×64×64	MP/s2	Pool 2×2	C dw/s1	3×3×256	C/s1	3×3×3×512
C dw/s1	3×3×64	C/s1	3×3×3×128	C/s1	1×1×256×512	MP/s2	Pool 2×2
C/s1	1×1×64×128	C/s1	3×3×3×128	C dw/s1	3×3×512		
C dw/s2	3×3×128	MP/s2	Pool 2×2	C/s1	1×1×512×512		
C/s1	1×1×128×128	C/s1	3×3×3×256	C dw/s2	3×3×512		
C dw/s1	3×3×128	C/s1	3×3×3×256	C/s1	1×1×512×512		
C/s1	1×1×128×256	MP/s2	Pool 2×2	MP/s2	Pool 2×2		
C dw/s1	3×3×256	C/s1	3×3×3×512	FC/s1	512×nClasses	FC/s1	512× nClasses
				Soft/s1	Classifier	Soft/s1	Classifier

Table 4: Differences of weights closer and further from the center. For lower layers, it clearly shows that magnitude of weights decrease with distance. (***) denotes a p-value < .001, ** < .01, * < .1)

Dataset	Architecture	All Layers		Lower $\frac{1}{2}$ Layers		Upper $\frac{1}{2}$ Layers	
		$m(I_c, I_n)$	$m(I_n, I_{co})$	$m(I_c, I_n)$	$m(I_n, I_{co})$	$m(I_c, I_n)$	$m(I_n, I_{co})$
ImageNet [pre-trained, from Keras]	VGG16	0.118***	0.077***	0.127***	0.113***	0.11***	0.042***
	ResNet50	0.069***	0.21***	0.026***	0.21***	0.112***	0.211***
	InceptionV3	-0.05***	-0.151***	0.083***	0.045***	-0.184***	-0.346***
	Xception	0.412***	0.04***	0.54***	0.408***	0.284***	-0.329***
	MobileNet	0.444***	0.553***	0.909***	1.093***	-0.022	0.013
	DenseNet121	-0.005**	-0.027***	0.074***	0.153***	-0.085***	-0.206***
CIFAR-100	VGG13(Table 3)	0.206***	0.273***	0.062***	0.036***	0.351***	0.51***
	ResNet18	0.164***	0.219***	0.106***	0.142***	0.222***	0.296***
	MobileNet(Table 3)	0.375***	0.552***	0.486***	0.626***	0.264***	0.479***

7.1 Testing for Locality

We tested the hypothesis that weights decrease with distance from the center. We used multiple common architectures trained on ImageNet and CIFAR-100 for 3×3 convolutions as shown in Table 4. Stars indicate whether the difference is significantly larger than 0 using a one-sided t-test. Our results for CIFAR-10 and FASHION-MNIST were qualitatively identical to CIFAR-100. While we focus on 3×3 convolutions due to their practical relevance, we also discuss 5×5 convolutions towards the end of the chapter. We denote the parameters of a network as follows. A convolution of a feature map w is a spatial matrix $w = (w_{i,j})$ of dimension $k \times k$ of width k and height k . A feature in a layer l consists of multiple $k \times k$ matrices, ie. one for each input feature (map). We denote by W_l the union of all $k \times k$ matrices of all features in layer l . We say that locality is supported, if a t-test deriving observations from each spatial matrix $w \in W_l$ yields significant results. More precisely, for each spatial matrix w we compute the means of weights at all distances from the center including distance 0, ie. the centers themselves. For a 3×3 matrix $w = (w_{i,j})$ with $i, j \in \{0, 1, 2\}$ we compute $m(w, I) := \sum_{(i,j) \in I} w_{i,j} / |I|$ for $I_c := \{(1, 1)\}$ and I_n, I_{co} as given in Equations 6.1. We define the difference in means for weights at varying distances by $s(w, I, I')$ (see Equations 7.1). An observation, ie. a spatial matrix w , is supportive of locality if sub-features closer to the center have larger weights, ie. $s(w, I_c, I_n) > 0$ and $s(w, I_n, I_{co}) > 0$. Since the differences might exhibit changing variances across layers, we divided by the standard deviation of $s(w, I, I')$ across all w of a layer l . The results in Table 4 state the mean across all observations for one network, ie. $m(I, I')$ defined below:

$$\begin{aligned}
 s(w, I, I') &:= m(w, I) - m(w, I') \\
 \sigma(W_l, I, I') &:= \sqrt{\frac{\sum_{w \in W_l} (s(w, I, I') - E[s(w, I, I')])^2}{|W_l|}} \quad \text{with } E[s(w, I, I')] := \frac{\sum_{w \in W_l} s(w, I, I')}{|W_l|} \\
 m(I, I') &:= \frac{\sum_{l, w \in W_l} s(w, l, I, I')}{\sum_{l, w \in W_l} |W_l|} \quad \text{with } s(w, l, I, I') := \frac{s(w, I, I')}{\sigma(W_l, I, I')}
 \end{aligned} \tag{7.1}$$

For lower layers there is consistent support for locality, but for higher layers it is mostly weaker or there is no support. One explanation is that down-sampling yields more abstract, semantically richer features with

less precise localization. Localization of features in upper layers might be less relevant, since the goal of classification is not localization. Strength estimation might also be more imprecise in upper layers.

Architectures with depth-wise separable planes (Xception [6] and MobileNet [14]) exhibit the largest degree of locality. Features extracted from a single feature map (as done for depth-wise separable convolutions) might be easier to localize. They might have clear maxima compared to feature maps that are a superposition of multiple features maps.

The reasons for the success of networks with shortcuts such as ResNet [13] or DenseNet [15] are mainly unclear. We might view the addition of the input X to the output $f(X)$ of a ResNet-block as “locality promoting”. The addition ensures that locations of large inputs will lead to large outputs. This is in alignment with locality, enforcing some degree of coherence between inputs and outputs, ie. if an input feature is large, it is likely that at the same location an output feature is centered.

We also used a VGG13 variant based on Table 3 for CIFAR-100, where we replaced all 3×3 convolutions with 5×5 convolutions for all layers with feature maps of width and height larger than the size of the convolution. We trained 20 networks and investigated $m(I, I')$ analogous as for 3×3 , ie. using I_c, I_n, I_{co} plus 3 additional index sets capturing elements at distance 2, ie. $I_2, \sqrt{5}$, ie. $I_{\sqrt{5}}$, and $\sqrt{8}$, ie. $I_{\sqrt{8}}$. We found for all 20 networks that $m(I_c, I_n) > 0$ and $m(I_n, I_{co}) > 0$ with all differences highly significant ($p < 0.001$). Also $m(I_{co}, I_2) > 0$ and $m(I_2, I_{\sqrt{5}}) > 0$ for 14 runs with $p < 0.01$. On the contrary if the difference was negative it was not significant at $p > 0.1$ for any occurrence except for $m(I_{\sqrt{5}}, I_{\sqrt{8}}) < 0$ for three runs. Overall, our experiments support the principle of locality in CNNs.

7.2 LOCO-REG Performance

We found that LOCO-REG with fixed parameters γ, η leads to improvements, but the parameters are cumbersome to set manually and gains are often only moderate. Table 4 suggests that the two parameters depend on the architecture, dataset and layer. To take this into account and ensure stability of parameters, we used layer-wise parameters (γ_l, η_l) , ie. (γ_l, η_l) are means per layer l for each architecture and dataset across all trained models (Table 6). The modulation function $a(r, c)$ (Table 6) is based on the rationale that the optimal parameters should be larger than the ones observed using uniform regularization. Overall, the modulation factor $c = 1.5$ performed best out of $c \in \{0.5, 1, 1.5, 2.5\}$. Optimizing c per architecture and dataset would give higher gains. Table 5 indicates that LOCO-REG on average improves test errors of all architectures on all datasets relatively about 2%, and from 0.1% up to 0.8% absolutely.

Table 5: Test errors for LOCO-REG
*** is a p-value $< .001$, ** $< .01$, * $< .1$

Dataset	Network	Standard Regular.	LOCO-REG
CIFAR-10	VGG13	6.26	6.13*
	ResNet18	5.29	5.18**
	MobileNet	11.01	10.64*
CIFAR-100	VGG13	27.13	26.31***
	ResNet18	25.61	25.15***
	MobileNet	36.3	35.49***
FASHION-MNIST	VGG13	5	4.9***
	ResNet18	4.65	4.54**
	MobileNet	5.84	5.73**

Table 6: LOCO-REG parameters (γ_l, η_l) per layer l

$$m(w, I) := \frac{\sum_{(i,j) \in I} w_{i,j}}{|I|} \quad \{\text{Mean of weights with indexes } I\}$$

Ratios for layer l averaged across trained models M :

$$r(M, l, I, I') := \frac{1}{|M|} \sum_{W_l \in M} \frac{\sum_{w \in W_l} m(w, I)}{\sum_{w \in W_l} m(w, I')}$$

$$a(r, c) := 1 + c(r - 1) \quad \{\text{Modulate deviations of } r \text{ from } 1\}$$

$$(\gamma_l, \eta_l) := (a(r(M, l, I_n, I_c), 1.5), \frac{1}{a(r(M, l, I_n, I_{co}), 1.5)})$$

8 Conclusions

The Principle of Locality is universal. In the context of representation learning it translates to “The inner parts (of features) matter more than the outer ones.” meaning that filters are preferable with larger weights near the center. It is supported by theoretical models as well as empirically. It can be exploited using non-uniform, spatial regularization leading to improvements of multiple architectures.

References

- [1] L. Barenboim, M. Elkin, S. Pettie, and J. Schneider. The locality of distributed symmetry breaking. *Journal of the ACM (JACM)*, 63(3):20, 2016.
- [2] Y. Bengio, A. Courville, and P. Vincent. Representation learning: A review and new perspectives. *IEEE transactions on pattern analysis and machine intelligence*, 35(8):1798–1828, 2013.
- [3] M. Bertalmío. Denoising of photographic images and video, 2018.
- [4] A. Bietti and J. Mairal. Invariance and stability of deep convolutional representations. In *Advances in Neural Information Processing Systems(NIPS)*, pages 6210–6220, 2017.
- [5] C.-Y. Chen, S.-C. Hwang, and Y.-J. Oyang. An incremental hierarchical data clustering algorithm based on gravity theory. In *Pacific-Asia Conference on Knowledge Discovery and Data Mining*, pages 237–250, 2002.
- [6] F. Chollet. Xception: Deep learning with depthwise separable convolutions. In *Conference on Computer Vision and Pattern Recognition (CVPR)*, pages 1800–1807, 2017.
- [7] A. Coates, A. Ng, and H. Lee. An analysis of single-layer networks in unsupervised feature learning. In *International conference on artificial intelligence and statistics(AIStats)*, pages 215–223, 2011.
- [8] T. Cohen and M. Welling. Group equivariant convolutional networks. In *International conference on machine learning*, pages 2990–2999, 2016.
- [9] M. Courbariaux, Y. Bengio, and J.-P. David. Binaryconnect: Training deep neural networks with binary weights during propagations. In *Advances in neural information processing systems(NIPS)*, pages 3123–3131, 2015.
- [10] R. C. Gonzalez, R. E. Woods, et al. Digital image processing, 2002.
- [11] B. Graham. Fractional max-pooling. *arXiv preprint arXiv:1412.6071*, 2014.
- [12] A. Hatamlou, S. Abdullah, and H. Nezamabadi-Pour. Application of gravitational search algorithm on data clustering. In *International Conference on Rough Sets and Knowledge Technology*, pages 337–346, 2011.
- [13] K. He, X. Zhang, S. Ren, and J. Sun. Deep residual learning for image recognition. In *Conference on computer vision and pattern recognition (CVPR)*, pages 770–778, 2016.
- [14] A. G. Howard, M. Zhu, B. Chen, D. Kalenichenko, W. Wang, T. Weyand, M. Andreetto, and H. Adam. Mobilenets: Efficient convolutional neural networks for mobile vision applications. *arXiv preprint arXiv:1704.04861*, 2017.
- [15] F. Iandola, M. Moskewicz, S. Karayev, R. Girshick, T. Darrell, and K. Keutzer. Densenet: Implementing efficient convnet descriptor pyramids. *arXiv preprint arXiv:1404.1869*, 2014.
- [16] M. Jaderberg, K. Simonyan, A. Zisserman, et al. Spatial transformer networks. In *Advances in neural information processing systems*, pages 2017–2025, 2015.
- [17] A. Krizhevsky and G. Hinton. Learning multiple layers of features from tiny images. Technical report, Citeseer, 2009.
- [18] B. M. Lake, T. D. Ullman, J. B. Tenenbaum, and S. J. Gershman. Building machines that learn and think like people. *Behavioral and brain sciences*, 40, 2017.
- [19] L. Liu, W. Ouyang, X. Wang, P. Fieguth, J. Chen, X. Liu, and M. Pietikäinen. Deep learning for generic object detection: A survey. *arXiv preprint arXiv:1809.02165*, 2018.

- [20] T. Mikolov, K. Chen, G. Corrado, and J. Dean. Efficient estimation of word representations in vector space. *Int. Conference on Learning Representations (ICLR)*, 2013.
- [21] J. Mutch and D. G. Lowe. Multiclass object recognition with sparse, localized features. In *Conference on Computer Vision and Pattern Recognition (CVPR)*, volume 1, pages 11–18, 2006.
- [22] L. Pessoa. Mach bands: How many models are possible? recent experimental findings and modeling attempts. *Vision Research*, 36(19):3205–3227, 1996.
- [23] P. Rodríguez, J. Gonzalez, G. Cucurull, J. M. Gonfaus, and X. Roca. Regularizing cnns with locally constrained decorrelations. *Int. Conference on Learning Representations (ICLR)*, 2016.
- [24] K. Simonyan and A. Zisserman. Very deep convolutional networks for large-scale image recognition. *Int. Conference on Learning Representations (ICLR)*, 2014.
- [25] J. T. Springenberg, A. Dosovitskiy, T. Brox, and M. Riedmiller. Striving for simplicity: The all convolutional net. *Int. Conference on Learning Representations (ICLR)*, 2014.
- [26] C. Szegedy, W. Liu, Y. Jia, P. Sermanet, S. Reed, D. Anguelov, D. Erhan, V. Vanhoucke, and A. Rabinovich. Going deeper with convolutions. In *Conference on computer vision and pattern recognition (CVPR)*, pages 1–9, 2015.
- [27] V. Thomas, E. Bengio, W. Fedus, J. Pondard, P. Beaudoin, H. Larochelle, J. Pineau, D. Precup, and Y. Bengio. Disentangling the independently controllable factors of variation by interacting with the world. *Advances in neural information processing systems(NIPS)*, 2018.
- [28] L. Wan, M. Zeiler, S. Zhang, Y. Le Cun, and R. Fergus. Regularization of neural networks using dropconnect. In *International Conference on Machine Learning (ICML)*, pages 1058–1066, 2013.
- [29] H. Xiao, K. Rasul, and R. Vollgraf. Fashion-mnist: a novel image dataset for benchmarking machine learning algorithms. *arXiv preprint arXiv:1708.07747*, 2017.
- [30] H. Zou and T. Hastie. Regularization and variable selection via the elastic net. *Journal of the Royal Statistical Society: Series B (Statistical Methodology)*, 67(2):301–320, 2005.